Passive Wireless Sensing for Unsupervised Human Activity Recognition in Healthcare

Wenda Li*, Yangdi Xu*, Bo Tan†, Robert. J. Piechocki*

*Department of Electronic and Electrical Engineering, University of Bristol, UK
†School of Computing, Electronics and Mathematics, Coventry University, UK
*{wenda.li, yangdi.xu, Robert. J. Piechocki}@bristol.ac.uk,†bo.tan@coventry.ac.uk

***Abstract*—Physical activity classification is an important tool for various applications such as activity of daily living (ADL) recognition and fall detection. Additionally, the non-contact nature of radar systems provides minimally invasive sensing platform. Doppler-based radar has been used for activity classification in the past. However, most of these studies considered supervised classification which requires labeled training data sets. In this paper, we propose a novel procedure of using micro Doppler radar for unsupervised classification with Hidden Markov Models (HMM). A low-complexity time alignment method for capturing activity is developed and an Elbow test has been adopted for model selection. Test results confirm the efficacy of the selected feature set and the proposed methodology. The results prove the proposed system can deliver a very good performance in ADL recognition tasks.**

***Index Terms*—Passive Sensing, Doppler Radar, Human Activity Recognition, Unsupervised Classification, HMM**

I. Introduction

Sixty percent of global deaths are related to Chronic Non-communicable Diseases (NCDs), which is expected to reach seventy-three percent by 2020 [1]. Physical inactivity is one of the major factors for NCDs that cause more than 2 million death each year. Thus, there is an increasing demand in human activity recognition in healthcare application [2]. Currently, device-free activity classification has gain more focus as it does not require any on-body sensor specially for the user with skin or Parkinson's disease. The video-based sensor has been widely used in activity classification [3], yet there are concerns about privacy and it is challenging in low-light situation. The work in [4] shows a potential in using acoustic detection sensor but this lacks in detection range. Alternatively, radar technique has the ability in long-term monitoring under almost all indoor condition and therefore can be applied without those limitations [5].

Many researchers have been used radar technique for studying human activity classification [6]–[8] with classifiers such as support vector machine (SVM), conditional random field (CRF) and latent Dirichlet allocation (LDA). However, in the situation when ground truth is not available, the above classifiers are not suitable since they require labeled data set for training purposes. From the application perspective, supervised classification requires the user to perform specified activity as training data. However, in reality, users normally perform unexpected, complex and various activity that those classifiers could not distinguish when detecting an unknown activity. In addition, for dangerous activity, user can hardly provide sufficient training for the supervised classifier that limits its application prospect in healthcare. We envisage that an unsupervised classifier could provide wider application potential as it can study the activity automatically and no training label is required. In this work, we purpose a HMM-based classifier with using of Doppler characteristics. The unsupervised classification is much more challenging than supervised classification as stated in [9] due to the reason that video-based system provides high dimensional data, whereas in our system the Doppler data is much scarce and lower dimension. Therefore we cannot directly use the HMM from work [3], [10] which build HMM for each individual activity, in comparison, we use one HMM to exam all activities by testing the difference in feature values and corresponding sequential relationship. The other reason is the difficulty in accessing obtained results, unlike supervised result, there is not a simple goal for analysis. We outline the method of calculating the classification rate and provide two different tests to present the performance. Note that, the labeled ground truth has only been used for interpreting the classification performance which does not affect training process.

In this work, we describe a procedure from collecting Doppler information to activity recognition with HMM. Firstly, we use cross ambiguity function (CAF) mapping [11] to extract Doppler information based on the reflected signal from target. Secondly, we purpose a low complexity time alignment method for Doppler spectrogram, so that the passive system could automatic capture an incoming activity. Moreover, HMM requires to define the hidden state, As there is no label on the data set, therefore the number of activity classes needs to be discovered. A novel algorithm has been present to estimate the class number by calculating the mean and variance of input data. Fourthly, initial matrix and transition matrix are two important parameters for HMM, yet they begin with random value due to the unlabeled data set. We use expectation maximization (EM) to improve those matrices to increase the classification accuracy. Compare to previous work [3], [8], [10], the following main contributions of the proposed system are presented:

- The proposed system does not require the user to provide

supervised activity for training and able to separate unlabeled data set. This function is more suitable and robust for e-Healthcare application.

- To the best of our knowledge, this is the first study of unsupervised learning with micro Doppler radar for activity classification. It is more challenging than previous work in [6], [8] and we show a novel procedure from collecting Doppler information to extract classification result.
- We also apply an Elbow test for solving the model selection problem of HMM. This method can be easily extended for other classification scenarios such as imaging, video.
- Five activities have been selected to evaluate the accuracy of proposed system. The classification accuracy is found to be around 72% with real measurements. The experimental results show a promising potential for the use of passive radar and HMM in unsupervised activity classification.

The rest of this paper is organised as follow: Section II presents the measurement of human activity including system description, Doppler spectrogram generation, and automatic time alignment; the HMM state estimation and graphic model used in our work are expressed in Section III; Section IV outlines two tests and corresponding results; Conclusion will be in Section V.

II. Measurement of Human Activity

We build a passive radar system based on our previous work [11] for collecting Doppler information. The passive system is based on a software-defined-radio (SDR) platform with real-time design. The system includes two NI USRP-2920 [12] for collecting signal. The system contains two antennas, one points to the energy harvesting transmitter [13] as the reference channel and other one points to the monitoring area as the monitoring channel. All measurements are conducted in a high cluster environment under line-of-sight condition. The detailed layout is explained in [11]. The block diagram of the signal processing is shown in Fig 1. The system includes two processes, the passive radar signal processing is implemented in LabVIEW^{TM}, whereas the classification part is implemented in Matlab. In future, we can convert both signal processing into one system.

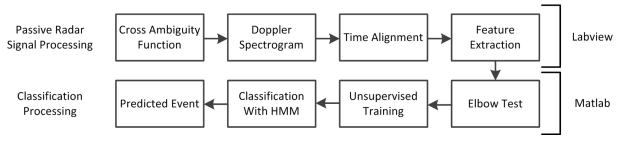

Fig. 1. Block diagram of the signal processing

During the measurement, A person was asked to perform no activity and five different activities in front of the monitoring antenna at range from 1-5 meters including, (a) no activity (standing still), (b) walking, (c) running, (d) jumping, (e) turning and (f) standing up from a chair. The total number of data set is (no activity) $\times$ (20 repetitions) + (5 activities) $\times$ (40 repetitions) = 220. The illustration of those activities are present in Fig 2.

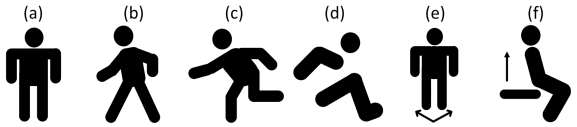

Fig. 2. Illustration of motion: (a) no activity (standing still), (b) walking, (c) running, (d) jumping, (e) turning and (f) standing up from a chair

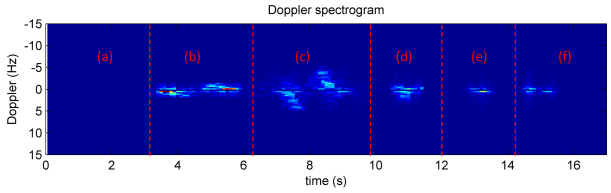

Fig. 3. Doppler spectrogram for no activity and five activities

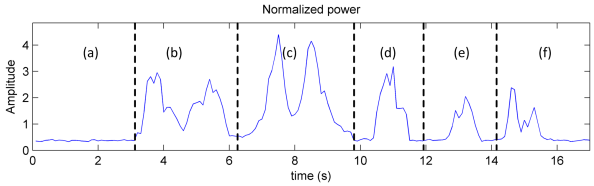

Fig. 4. Doppler power for no activity and five activities

A. Doppler Spectrogram Generation and Analysis

In this work, the cross ambiguity function (CAF) mapping has been used to extracting Doppler information from the reflected signal from person and generate corresponding spectrogram. The low-complexity CAF mapping can be expressed as (1):

$$CAF(\tau, f_d) = \sum_{k=0}^{n_b-1} \int_0^T S_i(t) R_i{}^*(t - kT_B - \tau) e^{jf_d(t)} dt \quad (1)$$

where τ is the propagation delay, f_d is the Doppler shift. T_B is the batch length, n_b is the number of batches, k is the index of batching, S_i and R_i is the obtained signal from monitoring & reference channel with batch process. A Doppler spectrogram $D(f_d, n)$ is then generated based on a group of CAF mapping by selecting the column that containing the max Doppler peak. Currently, the system is able to output one Doppler spectrogram every 0.1 seconds. The above signal processing are briefly described in our previous work [11].

We plot the Doppler spectrogram for no activity and five activities in Fig 3. The Doppler trace in Fig 3 represents the Doppler shift of torso. This is because of torso gives much stronger reflection compare to other parts of the body. As a result, the Doppler shift of torso will cover the Doppler shift from other parts of the body. Also for activity such as (e) and (f), the Doppler shift of head and arms are comparably short duration or even same as the torso. For both activity (b) and (c), we had the person moving in both directions, so they have both positive and negative Doppler shift across the duration.

The short activity such as (d), (e) and (f) contains Doppler shift at both positive and negative domain. This is because of during these activities, part of the body moves towards the antenna, yet other part moves away from the antenna. For long activity such as (b) and (c), the major Doppler shift are mostly concentrated in one domain as the whole body is either towards or outwards from the antenna.

B. Time Alignment

One challenge of unsupervised classification is the process of detecting a change point. As there is no label of the start point of activity, thus the passive system should capable of automatic identifying the inactive and active period. The traditional method such as manifold alignment and dynamic time wrapping (DTW) [14] constraint the general problem to high-dimensional vectors and therefore require high computational power which is not an ideal solution for our system. In comparison, We transform this challenge into a pulse detection problem by calculating the power intensity in Doppler spectrogram.

We plot the Doppler power for no activity and five activities in Fig 4 corresponding to the Doppler spectrogram in Fig 3. As can be seen, the peaks of each activity are clear and distinct. We set the reference level at 10% of the waveform amplitude to detect the start point and duration of activity. 97.3% (214 out of 220) accuracy has been observed between the inactivity and activity period. The figure also shows the Doppler power of running is higher than other activities as expected. This is because of high Doppler activity gives wider bandwidth in the spectrogram and therefore results in higher power.

C. Feature Extraction

Although the Doppler spectrogram itself can be used for classification without any feature extraction. However, the high dimensional data requires high computational power; thus we need to reduce the data dimension while maintaining the characteristics of the Doppler spectrogram. Currently, the singular value decomposition (SVD) is a popular tool for eigenvector based features. However, SVD requires high dimensional signature data for testing, and the Doppler spectrogram in this work is not sufficient to be extracted by SVD. By this purpose, a database is generated for five different activities. In addition, to further improve the automation of the system, the feature extraction in our system is prior designed. Consider the feature extraction method for micro-Doppler in [6], we select following six features:

(1) the duration of the activity
(2) the maximum upper Doppler shift of the activity
(3) the maximum lower Doppler shift of the activity
(4) the peak-to-peak bandwidth of Doppler
(5) the mean power of the activity
(6) the standard deviation of the power of the activity

The duration of the activity (1) is a basic and important information to describe an activity since the time to complete each activity is intuitive different. The maximum upper/lower Doppler shift of the activity (2)/(3) represents the maximum speed towards/outwards to the antenna. They outline the maximum detected speed by passive radar and very useful for identified the activity. The peak-to-peak bandwidth of Doppler (4) shows the difference between maximum positive and negative Doppler shift that gives the background information about the action of torso. The mean power of the activity (5) gives the average power during an activity's period. And it is very useful as fast activity gives higher power than that from a slow activity. The standard deviation of the power of the activity (6) is chosen for the similar reason as (5). The mean values of each feature from all five activities are present in Table I. As it can be seen, there are differences among each activity that can be potentially used for classification purpose. The effectiveness of above features will be shown at Section IV-A.

TABLE I
MEAN VALUES OF FEATURES

activity \ feature	(1)	(2)	(3)	(4)	(5)	(6)
(b)	2.5	9.9	6.3	16.2	55.2	2308.9
(c)	2.6	13.6	14.2	27.8	131.5	2542.5
(d)	1.4	7.1	6.5	13.3	68.1	1388.0
(e)	0.8	5.8	5.3	11.1	21.6	782.6
(f)	1.2	5.6	5.4	10.9	27.4	1173.3

III. HIDDEN MARKOV MODEL

Hidden Markov model is one of the most popular statistical models for recognition/categorization [9]. There are two types of states: observation state and hidden state, which includes extracted feature and action state respectively. The connection between each state can be described as a joint probability distribution over the observation space. We present our HMM using a graphical model and its dependencies between different activities using transition matrices.

A. Estimate Number of Class

Since our work emphasis on unsupervised training, we assume we have no knowledge of the data set. Therefore, rather than manual assign the number of activity state to the hidden node, we use K-mean clustering together with the 'Elbow Test' to estimate the optimal number of clusters. In addition, the number of cluster leaves indicates the total number of hidden states for our HMM model. The equation of the Elbow test can be expressed as (2):

$$R_k = \frac{\sum_{i=1}^{k}\sum_{j=1}^{l}|(Y_{i_j} - \overline{Y}_i)|}{\sum_{i=1}^{k-1}|(\overline{Y_i} - \overline{Y}_{i+1})|} \tag{2}$$

where, k is the number of clusters, l is the number of data point within a specific cluster and Y is the matrix contains extracted feature from Table I. The range of k is from 2 to 10, for each k, R is obtained by calculating the sum of intra-cluster distances over the sum of inter-cluster distance.

Fig 5 shows the Elbow test based on the features from Doppler spectrogram. The figure shows the value of R (the

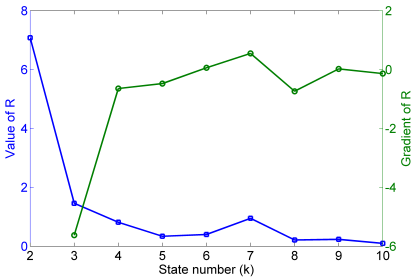

Fig. 5. Elbow test on Doppler features

blue line) generally decreases as state number (k) increases. However, the optimal number of clusters is determined where the value of R start to become relatively consistent. This is computed by calculating the gradient between R_k and R_{k+1} (the green line). We know that to determine the optimum number of clusters, the intra-cluster distance should be minimized and the inter-cluster distance should be maximized. The value of R should keep decreasing until it reaches the optimum point. Thus, there are three conditions for determining the optimum value of cluster k.

- Condition one: gradient of k_i should be smaller than k_j given $i < j$
- Condition two: k_i should be the optimum value if the gradient of k_{i+1} is greater than zero
- Condition three: all k value after k_{i+1} is ignored if k_{i+1} is greater than zero

The last condition is because a positive gradient indicates k-mean clustering is deviating from the optimal point. Therefore, according to Fig 5, $k = 5$ is selected from Elbow test and it matches the number of activity in this work. We also evaluate the accuracy of the Elbow test by randomly remove some data set from Elbow test, and we observe 92% in correctly detect five activities.

B. HMM Graphic Model and Classification Process

We use an HMM model for our activity classification problem. The example of graphical representation is in Fig 6. A_t and A_{t+1} are the two discrete hidden nodes which represent different activity states. O_t and O_{t+1} are the corresponding observation nodes which contains six features in our case. In this study, Murphy's HMM toolbox [15] has been used for implementation.

The training of HMM requires defining the initial state matrix Q, which is the probabilities of each activity state at A_t; and the state transition matrix S, which is the probability of each activity at A_{t+1} given A_t. However, in unsupervised learning, the label of the data set is not known and therefore we are unable to obtain the initial state matrix and state transition matrix. Thus, firstly, both matrices Q_0 and S_0 are randomly initialized which is the input for the hidden nodes. The sum of Q_0 is equal to one and S_0 has the structure of the stochastic matrix. Secondly, Expectation Maximization (EM) is used as the optimization tool for initial state and state transition matrices. It performs an expectation (E) step, by

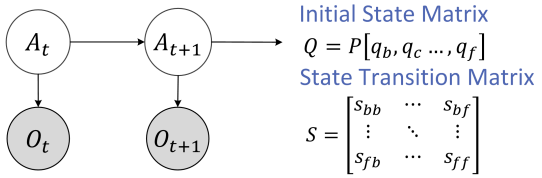

Fig. 6. An example of HMM structure with initial state matrix and state transition matrix

creating a function for expectation of current estimation, and a maximization (M) step, by computing the maximized expected log-likelihood found on E step. In this work, ten iterations are selected to reach the maximum limitation. Finally, we have the optimized matrix Q_1 and S_1 to calculate the mixture probability of the testing data. The output probability sequence can then be recovered by finding the most probable path with Viterbi decoder.

IV. Classification Result

Unsupervised classification often contains fluctuation and difficulty in accessing its result [4]. In the case of HMM, there are three factors that need to be noticed. The first factor is that both matrix Q_0 and S_0 are set to be random which means the optimized matrix Q_1 and S_1 can be varied even within same training set and training order (no label on training set). To reduce this fluctuation and improve the certainty of the obtained result, we carry out the test with following rules: (1) 40 recordings from each activity are used, 30 for training set and 10 for testing set (2) testing set can not overlap with training set; (3) 4 tests with different combinations, for example, 1-10 as testing sets whereas the others as training sets, then 11-21 as testing sets whereas the others as training sets and so on (4) matrix Q_0 and S_0 are generated randomly for once, then keep using these matrices for every test so that we can assume all test are within one instance.

The second factor is the order of the training set. We know there is an interconnection between different activity [3], which means a person does not perform activity randomly but instead a series of related activity. Therefore the order of training set is essential for determining the state transition matrix in HMM. In this work, we carefully simulate the training order in each test to present the classification result (will be explained in each test).

Furthermore, another factor for unsupervised HMM classification is the way of interpreting result. The problem in this work is the training state number does not directly relate to the desired state number. For example, state ***b*** could be assigned to any state after the training that results in a variation in state to state connection. To avoid this mismatch, we extract the probability from Viterbi path and compare with the ground truth label. The purpose of this process is for explaining the result only and it is not including in either training and testing of the HMM. For a real application, this process is not necessary as the system only needs to provide state connections for real activity.

A. Effectiveness of Selected Feature

In the first test, we investigate which feature plays the most important role in the classification. For this test, we set the training order as following: first 30 training sets are activity (b) then 30 training sets are activity (c) and so on. This order assumes the user perform same activity repeatedly, and it contains very few state transition (only happens when switching to next activity) so that the test on each feature is mainly based on itself. Also, the state transition and initial state matrix are calculated with labeled training set as we only test the effectiveness of feature in this test. The accuracy rate of each feature is present in Table II. As it can be seen, the sequence of feature in terms of accuracy is shown as:(5), (1), (6), (3), (2) and (4). The mean power (5) alone gives more than half accuracy rate at 60% as the result of large diversity across each activity; the maximum upper Doppler shift (4) gives only 32% due to the value in activity (d), (e), (f) are very closed; the duration (1) gives second best accuracy rate at 56% as it provides good separation between long and short activity, yet less effective in similar length activity. Note that, we observed the test on feature (2), (3), (4) occasionally output Inf values for Q_1 and S_1 that create errors in HMM. This failure indicates the input feature is not sufficient for separating those activities and more feature is required.

TABLE II
CLASSIFICATION ACCURACY OVER EACH SINGLE FEATURE

Feature	(1)	(2)	(3)	(4)	(5)	(6)
Accuracy	56%	32%	39%	36%	60%	52%

Then we calculate the combined accuracy rate of these features by adding one at a time with the sequence of (5), (1), (6), (3), (2) and (4). The combination shows the improvement of each feature versus the classification accuracy. As can been in Table III, as expected, accuracy increased with the number of features. The highest accuracy rate has occurred when all six features are applied at 89%. For the last two features, the bandwidth of Doppler (4) and maximum upper Doppler shift (2), the improvement is very limited (only 2%) compare to the first four features. It shows the current six features are sufficient for classification, and good accuracy could be achieved with only four features (5), (1), (6), (3).

TABLE III
CLASSIFICATION ACCURACY WITH INCREASING NUMBER OF FEATURE

Number of Feature	1	2	3	4	5	6
Accuracy	60%	73%	79%	87%	88%	89%

B. Classification and Simulation of Real Scenario

The training order in Section IV-A can only present the activity under experiment scenario, as the user can hardly perform same activity repeatedly in a short period of time. Therefore, we need a more realistic training order to test the HMM performance. For this purpose, two variables need to be defined for simulating the training order: state number (represent the order of activity) and the feature number. In this work, a pre-set state transition matrix is build referred to the simulation model in [16] as shown in Table IV. The state number is then selected randomly but based on the distribution of the pre-set state transition matrix so that we can evaluate the classification performance in a more realistic scenario. Different person could have variation in number of activity or percentage in state transition matrix (represent his/her life style). It can be simply convert into this model by filter out the inactivity period with the time alignment method explained earlier so that only activities are recorded, then use the Elbow test to decide the size of state transition matrix. In the case of continuous activity (no time gap between two activities), we could use the activity segmentation method [3], [17] to separate different activity.

TABLE IV
PRE-SET STATE TRANSITION MATRIX

State Transition Matrix (S_1)	State b	State c	State d	State e	State f
State b	0.04	0.65	0.03	0.12	0.16
State c	0.11	0.10	0.70	0.07	0.02
State d	0.43	0.22	0.27	0.08	0.03
State e	0.22	0.06	0.08	0.57	0.07
State f	0.04	0.17	0.03	0.03	0.73

TABLE V
ESTIMATED STATE TRANSITION MATRIX

State Transition Matrix (S_1)	State b	State c	State d	State e	State f
State b	0.09	0.58	0.04	0.11	0.18
State c	0.12	0.23	0.61	0.02	0.02
State d	0.37	0.33	0.15	0.11	0.04
State e	0.34	0.02	0.12	0.45	0.06
State f	0.14	0.23	0.04	0.08	0.51

The feature number is then picked up randomly from the corresponding activity so that we could further improve the randomness. In Table V, we provide an example of estimated state transition matrix S_1 after training with 250 data sets. As can be seen, the percentage in each state have some variations but closed value compares to that in Table IV. This is because of the HMM contains error in match training set during the EM process. Table IV can be also considered as the transition matrix obtained from a supervised method. The variation between Table IV and V shows the difference between supervised and unsupervised study.

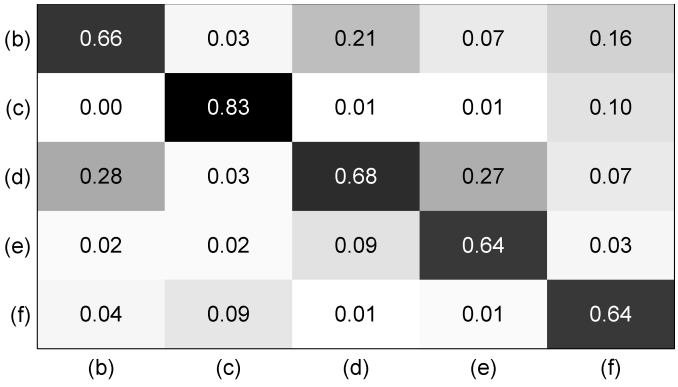

Fig. 7. Confusion Matrix

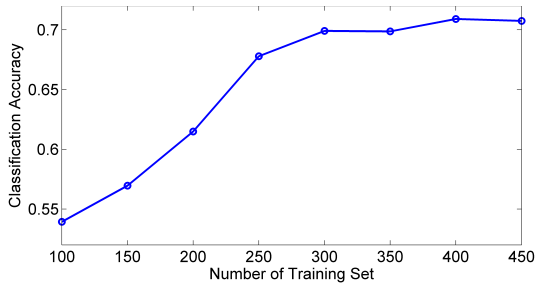

Fig. 8. Classification Accuracy Versus Number of Training Set

The averaged classification result is shown in Fig 7. As it can be seen, the overall accuracy is 69% which drops dramatically compares to test A (89%). This is because of the training set contains much complicated state transition that introduces uncertainty in EM process. Also, the optimized state transition matrix in this test contains error which further reduces its accuracy. Activity (c) has the highest classification rate at 83%; we believe it benefits from the longer duration that provides more diversity features than other activities as shown in Table I. Activity (b), (d), (e), (f) all have similar rate at around 65%.

It is also worth to explore the effect of number of training set to the accuracy. As each feature is selected randomly so that we can have more data set in training. We measure the length of training set from 100 to 450 and plot the related accuracy rate in Fig 8. As can be seen, the accuracy reaches 70% with 300 training set and has little improvement until 450 training set that shows the limitation of current system at around 72%. One of the possible solution to increase the accuracy is adding more monitoring channel to increase feature diversity. Compare to the supervised Doppler study in work [7] (85.3%) and [6] (92.8%), our work has some degradation in accuracy but more robust for a real application.

V. Conclusions

In this paper, we present a novel unsupervised classification system by using the passive radar. The HMM classification results show that the passive radar is an ideal solution for eHealthcare application to identify the human activity and situation. The proposed time alignment method in Section II-B has been shown a sufficient detection between inactivity and activity period. A K-means based algorithm has been carried out with Elbow test in Section III-A to estimate the number of activity class, and shown the correct number of desired class. We also present the structure of HMM where use activity as hidden node and Doppler information as observation node. By leveraging EM algorithm, the system is able to separate the unlabeled training data and estimate the hidden sequential relationship. The experiment result shows 69% accuracy rate with 250 training set and 72% is considered as the limitation of current system.

The future work will include a long-term monitoring period to obtain real life data for evaluating the proposed passive radar system. Current work assumes the activity within a certain state transition matrix, however, in real life it may contain more activities and variations. The long-term activity data could provide detailed relationship between different activity so that we could better exam the proposed methodology. Additionally, it may be worth to expand current system with multiple monitoring channels. The additional monitoring channel can provide more diversity feature that further improves the classification accuracy.

Acknowledgment

This work was partially funded under the SPHERE IRC, the UK Engineering and Physical Sciences Research Council (EPSRC), Grant EP/K031910/1.

References

[1] World health report 2002. [Online]. Available: http://www.who.int/whr/2002/en/whr02_en.pdf

[2] T. Choudhury, G. Borriello, S. Consolvo, D. Haehnel, B. Harrison, B. Hemingway, J. Hightower, P. . Klasnja, K. Koscher, A. LaMarca, J. A. Landay, L. LeGrand, J. Lester, A. Rahimi, A. Rea, and D. Wyatt, "The mobile sensing platform: An embedded activity recognition system," *IEEE Pervasive Computing*, vol. 7, no. 2, pp. 32–41, April 2008.

[3] M. Brand and V. Kettnaker, "Discovery and segmentation of activities in video," *IEEE Transactions on Pattern Analysis and Machine Intelligence*, vol. 22, no. 8, pp. 844–851, Aug 2000.

[4] D. Cournapeau, S. Watanabe, A. Nakamura, and T. Kawahara, "Online unsupervised classification with model comparison in the variational bayes framework for voice activity detection," *IEEE Journal of Selected Topics in Signal Processing*, vol. 4, no. 6, pp. 1071–1083, Dec 2010.

[5] W. Li, B. Tan, R. J. Piechocki, and I. Craddock, "Opportunistic physical activity monitoring via passive wifi radar," in *e-Health Networking, Applications and Services (Healthcom), 2016 IEEE 18th International Conference on*, Sep 2016.

[6] Y. Kim and H. Ling, "Human activity classification based on micro-doppler signatures using a support vector machine," *IEEE Transactions on Geoscience and Remote Sensing*, vol. 47, no. 5, pp. 1328–1337, May 2009.

[7] J. D. Bryan, J. Kwon, N. Lee, and Y. Kim, "Application of ultra-wide band radar for classification of human activities," *IET Radar, Sonar Navigation*, vol. 6, no. 3, pp. 172–179, March 2012.

[8] M. B. Abidine and B. Fergani, "Evaluating c-svm, crf and lda classification for daily activity recognition," in *Multimedia Computing and Systems (ICMCS), 2012 International Conference on*, May 2012, pp. 272–277.

[9] G. James, D. Witten, T. Hastie, and R. Tibshirani, *An Introduction to Statistical Learning with Applications in R*. Springer New York, 2014.

[10] M. O. Padar, A. E. Ertan, and . . Candan, "Classification of human motion using radar micro-doppler signatures with hidden markov models," in *2016 IEEE Radar Conference (RadarConf)*, May 2016, pp. 1–6.

[11] W. Li, B. Tan, and R. J. Piechocki, "Non-contact breathing detection using passive radar," in *2016 IEEE International Conference on Communications (ICC)*, May 2016, pp. 1–6.

[12] Ni usrp 2921. [Online]. Available: http://sine.ni.com/nips/cds/view/p/lang/en/nid/212995

[13] Powercast energy harvesing transmitter. [Online]. Available: http://www.powercastco.com/products/powercaster-transmitter

[14] S. Masood, M. P. Qureshi, M. B. Shah, S. Ashraf, Z. Halim, and G. Abbas, "Dynamic time wrapping based gesture recognition," in *Robotics and Emerging Allied Technologies in Engineering (iCREATE), 2014 International Conference on*, April 2014, pp. 205–210.

[15] Hidden markov model (hmm) toolbox for matlab. [Online]. Available: https://www.cs.ubc.ca/ murphyk/Software/HMM/hmm.html

[16] A. Elbayoudi, A. Lotfi, C. Langensiepen, and K. Appiah, "Modelling and simulation of activities of daily living representing an older adult's behaviour," in *Proceedings of the 8th ACM International Conference on PErvasive Technologies Related to Assistive Environments*, ser. PETRA '15. New York, NY, USA: ACM, 2015, pp. 67:1–67:8. [Online]. Available: http://doi.acm.org/10.1145/2769493.2769544

[17] G. Zhang and M. Piccardi, "Structural svm with partial ranking for activity segmentation and classification," *IEEE Signal Processing Letters*, vol. 22, no. 12, pp. 2344–2348, Dec 2015.